Electronic Supplementary Information (ESI)

Three-dimensional Macroporous Graphene Architectures as High Performance Electrodes for Capacitive Deionization

Hui Wang,[a,b] Dengsong Zhang,*[a] Tingting Yan,[a] Xiaoru Wen,[a] Jianping Zhang,[a] Liyi Shi*[b] and Qingdong Zhong[b]

[a] *Research Center of Nano Science and Technology, Shanghai University, Shanghai 200444, China. Fax: 86 21 66136079; E-mail: dszhang@shu.edu.cn*

[b] *School of Material Science and Engineering, Shanghai University, Shanghai 200072, China. E-mail: shiliyi@shu.edu.cn*

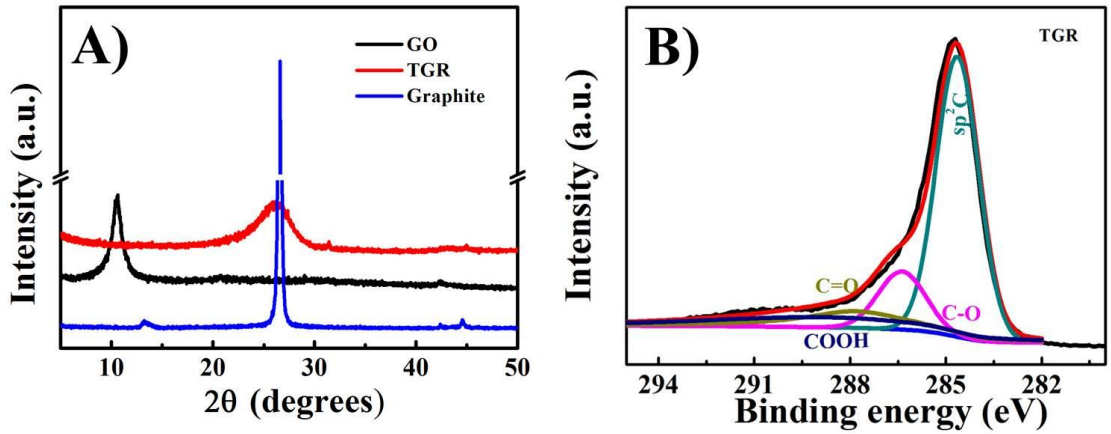

Fig. S1 (A) XRD patterns of TGR, GO and graphite, and (B) XPS spectrum of TGR.

For comparison, the XRD pattern of TGR is shown in the Figure S1A. Compared to GO, the sharp peak at 10.3°disappears, while a board peak at 2θ=23.2° appears in the XRD pattern of TGR. Hence, the oxygen-containing groups on the GO planes are removed after the high temperature calcination.[1] As seen obviously, the peak at 23^{o} is strong, indicating the exfoliation degree of GO is compromised in the absence of PS templates. During the calcination process, graphene sheets in the TGR stacks compactly due to the strong π-πconjugated structure and van der Waals force between the planer basal planes of graphene sheets. Oppositely, gases released from the pyrolysis of PS templates have promoted the exfoliation of graphene sheets and form

numerous open pores in the 3DMGA structure.[2, 3] Therefore, the 3DMGA exhibits more sufficient exfoliation as compared with the TGR. In Figure S1 B, the C1s spectrum of TGR includes four main peaks centered at 284.6, 286.4, 287.8 and 288.8 eV. Noticeably, the intensity of oxygen functionality peaks in the C1s XPS spectrum is weak, indicating that GO was highly reduced after the high temperature calcination. However, we can conclude that the reducing degree of TGR is similar to 3DMGA after the calcination with the same conditions, but the exfoliation is deeply compromised according to the analysis of XRD and XPS.

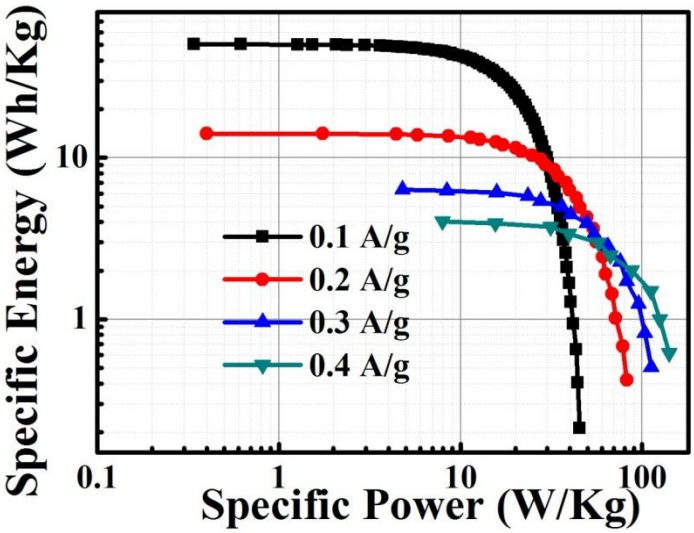

Fig. S2 Ragone Plots of 3DMGA electrodes at various current densities.

Ragone Plots in the Figure S2 shows the relationship between the special energy and the special power density for various current loads from 0.1—0.4 A g^{-1}. It is clear that higher current loads lead to an increased power output. The 3DMGA has a power density of 45.34 W Kg^{-1}, while the current density was raised up to 0.4 A g^{-1}, the power density is increased to 141.12 W Kg^{-1}. Meanwhile, the decrease in the special energy at the low current load is less rapid than that at the high current, indicating the 3DMGA electrode exhibits the typical hook shape of Ragone plot.[4]

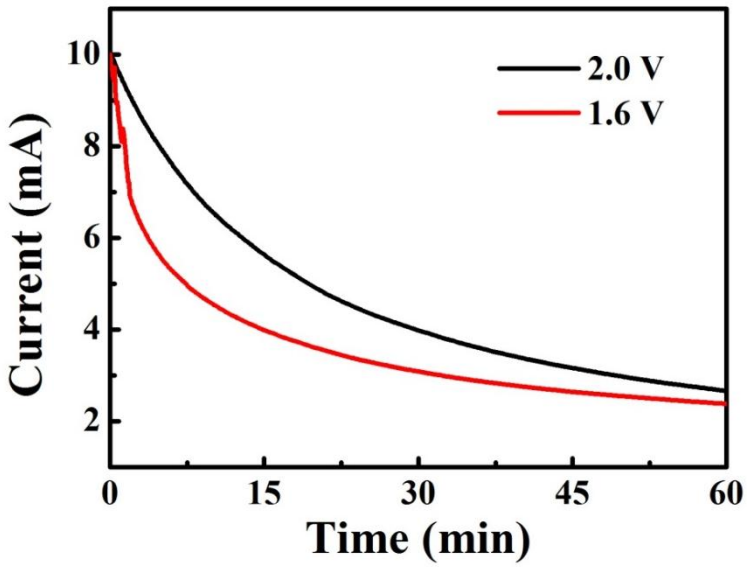

Fig. S3 Plots of current *vs* time during the CDI process for the 3DMGA electrode in NaCl solution with an initial conductivity of 107 μS cm^{-1}.

As shown in the Fig. S3, the current drop rapidly with time during the CDI application at an applied voltage of 2 V and 1.6 V and the current response is found to be proportional to the applied voltage. In addition, the curve under 2 V shows a similar tendency with that under 1.6 V, indicating that no water electrolysis was taking place. Ideally, if each electron charge is fully balanced by ion adsorption, the transfer of electron could be monitored and the thus current response is generated accordingly. Therefore, more ions in the salty solution are adsorbed by the electrode at a high voltage according to the current response curve.[5-7]

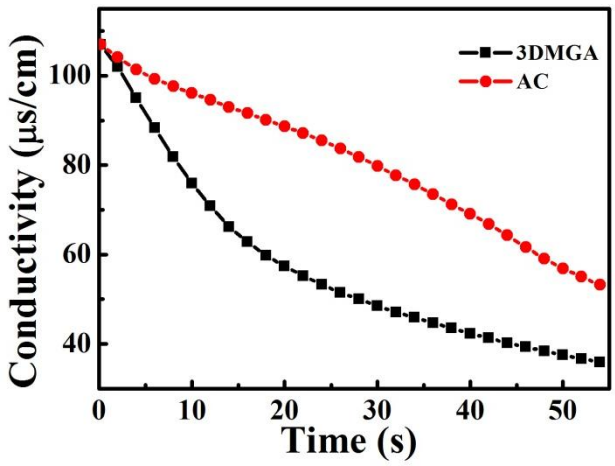

Fig. S4 CDI profiles of the 3DMGA and commercial activated carbon (AC) electrodes under 1.6 V

For comparison, the CDI performance of AC electrode is measured under the same batch-mode experiment conditions as the 3DMGA one. As seen the CDI curves in the Fig. S4, the solution conductivity by using AC electrodes is always higher than that of 3DMGA during the whole adsorption process, indicating the AC exhibits a lower deionization rate due to the existence of micropores.[8, 9] The electrosorption capacity of AC is 2.9 mg /g, which is lower than that of the 3DMGA one (3.9 mg/g).

References

1. C. M. Chen, J. Q. Huang, Q. Zhang, W. Z. Gong, Q. H. Yang, M. Z. Wang and Y. G. Yang, *Carbon*, 2012, **50**, 659-667.
2. J. F. Shen, T. Li, Y. Long, M. Shi, N. Li and M. X. Ye, *Carbon*, 2012, **50**, 2134-2140.
3. Y. X. Xu, Z. Y. Lin, X. Q. Huang, Y. Liu, Y. Huang and X. F. Duan, *ACS Nano*, 2013, DOI: 10.1021/nn4000836.
4. Z. Peng, D. S. Zhang, L. Y. Shi and T. T. Yan, *J Mater Chem*, 2012, **22**, 6603-6612.
5. H. B.Li, L. K. Pan, C. Y.Nie, Y.Liu and Z. Sun, *J Mater Chem*, 2012, **22**, 15556-155561.
6. H. B. Li, T. Lu, L. K. Pan, Y. P. Zhang and Z. Sun, *J Mater Chem*, 2009, **19**, 6773-6779.
7. H. Li, S. Liang, J. Li and L. He, *Journal of Materials Chemistry A*, 2013, **1**, 6335-6341.
8. H. B. Li, L. K. Pan, T. Lu, Y. K. Zhan, C. Y. Nie and Z. Sun, *J Electroanal Chem*, 2011, **653**, 40-44.
9. L. D. Zou, L. X. Li, H. H. Song and G. Morris, *Water Res*, 2008, **42**, 2340-2348.